ISSN 0006-3509, Biophysics, 2019, Vol. 64, No. 4, pp. 533–542. © Pleiades Publishing, Inc., 2019.
Russian Text © The Author(s), 2019, published in Biofizika, 2019, Vol. 64, No. 4, pp. 674–685.

MOLECULAR BIOPHYSICS

Intracellular Localization and Phototoxicity Mechanisms of Chlorin e_6 Derivatives and Their Liposomal Formulations

T. E. Zorina[a], *, I. V. Yankovsky[a], I. V. Yakovets[a], I. E. Kravchenko[a], T. I. Ermilova[b], T. V. Shman[b], M. V. Belevtsev[b], and V. P. Zorin[a]

[a] *Belarusian State University, Minsk, 220030 Republic of Belarus*
[b] *Belarusian Research Center of Pediatric Oncology, Hematology, and Immunology, der. Borovlyany, Minsk oblast, 223053 Republic of Belarus*
**e-mail: zorinate@mail.ru*

Received January 16, 2019; revised January 16, 2019; accepted March 5, 2019

Abstract—Confocal microscopy and colocalization analysis using Pearson correlation coefficients were used to show that esterified chlorin e_6 derivatives and their liposomal forms are mainly localized in the endoplasmic reticulum, Golgi complexes, cell mitochondria, and levels of their localization in lysosomes are low. Cellular uptake and accumulation kinetics of chlorin e_6 derivatives were strongly depended on the type of pharmacological formulation used for photosesitizers administration, while intracellular localization was independent on the formulation. Differences in the photodynamic activity and sensitization mechanisms for chlorin e_6 derivatives and their liposomal forms were shown when compared to those of chlorin e_6 photosensitizers in K562 cells. It is assumed that the observed differences in the mechanisms of cellular damage are to a greater extent due to specific photosensitizer localization.

Keywords: chlorin e_6 derivatives, liposomal formulations, intracellular localization, cytotoxicity, apoptosis
DOI: 10.1134/S0006350919040250

A photodynamic effect on cells and tissues in the presence of photosensitizers (PSs) is achieved by the participation of free radical reactions and reactive oxygen species. Singlet oxygen ($^1O_2$) is the main agent involved in photosensitized oxidation in the presence of a series of porphyrin-based PSs [1, 2]. The efficiency of photodamage of biological systems is directly linked to PS localization because the $^1O_2$ lifetime is short (~0.03–0.04 μs) and the diffusion distance during this time period is no greater than 0.1 μm from the generation spot [1, 3]. The cell structures in which PSs accumulate are the primary targets of an oxidative action of PSs; thus, the intracellular PS localization significantly influences the mechanism of cell damage.

The accumulation and distribution of PSs in various cells and tissues strongly depend on their physical, chemical, and structural properties. The presence of either cationic or anionic groups and symmetry in the arrangement of porphyrin side substituents significantly affect the interaction of PSs with the cell and tissue structures and influence the localization and accumulation of the PS molecules [4, 5].

It had been shown that chlorin e_6 (Chl e_6) and the Chl e_6 ester derivatives (DChl e_6) dimethyl (DME) and trimethyl esters (TME) of Chl e_6 can find applications in photodynamic therapy, including for the treatment of cancer, vascular disease, and selective damage of cells with increased proliferation [5, 6]. The low solubility of these compounds in an aqueous medium necessitates the use of special carriers for their administration. Nanoscale lipid vesicles are the most common pharmaceutical formulation that is used for administration non-polar drugs [7, 8]. However, the use of liposomal forms (LFs) to deliver PSs requires more investigation because the characteristics of the resultant product depend not only on the properties of the PS itself, but also on the structural characteristics of nanoscale lipid vesicles.

In this paper, we have evaluated the specificity of interaction between chlorins and cultured cells and the effect of the chemical structure and formulations that are used to administer the PS on this interaction. The localization and accumulation of Chl e_6 in K562 cultured cells and its ester derivatives that were administrated to cell suspension in organic solvents or in LFs were studied by confocal fluorescence microscopy and

Abbreviations: PS, photosensitizer; Chl e_6, chlorin e_6; DChl e_6, esterified derivatives of chlorin e_6; DME, dimethyl ester of chlorin e_6; TME, trimethyl ester of chlorin e_6; LF, liposomal form; DMPC, dimyristoyl phosphatidylcholine, FCS, fetal calf serum; PCC, Pearson correlation coefficient; CMXRos, chloromethyl-X-rosamine.

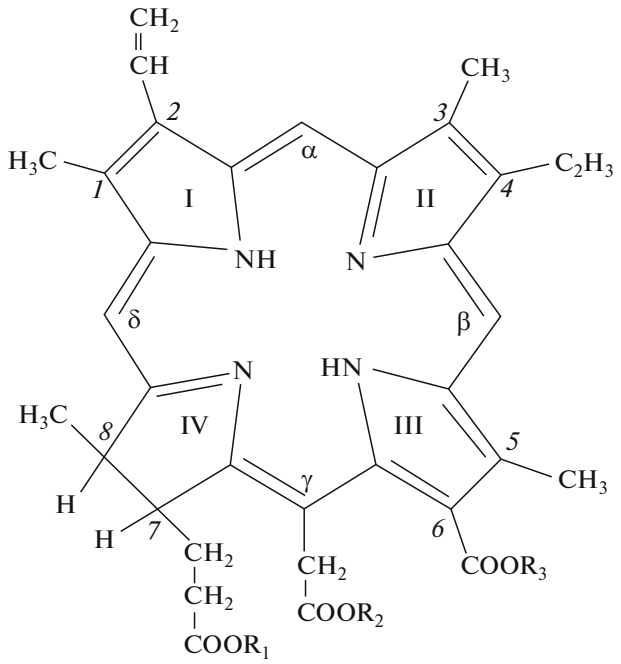

Fig. 1. The structural formulas for chlorin e_6 and its derivatives: Chl e_6 $R_1 = R_2 = R_3 = H$; DME $R_1 = H$, $R_2 = R_3 = CH_3$; TME $R_1 = R_2 = R_3 = CH_3$.

cytometry. The mechanisms of cellular destruction by chlorin photosensitizers and their LFs were analyzed.

MATERIALS AND METHODS

Photosensitizers and their liposomal formulations. Chlorins were synthesized according to the Fischer and Orth method [9] with modifications. To synthesize esterified derivatives of Chl e_6, DME, and TME, pheophytin or Chl e_6 were used as starting materials. The purity of Chl e_6 and its derivatives was checked chromatographically. The structural formulas of the studied chlorins are shown in Fig. 1.

Liposomes loaded with chlorins at a certain lipid–pigment ratio were prepared from synthetic saturated lipid dimyristoyl phosphatidylcholine (DMPC) (Sigma, United States) in an Avanti miniextruder (Bingham method), using 100 nm Nuclepore polycarbonate membrane filters (Whatman, United Kingdom). Photosensitizers were loaded into lipid vesicles at the step of lipid film preparation. The dried lipid film was hydrated with a Dulbecco's phosphate-buffered salt solution (pH 7.4) with constant stirring. The extent of Chl e_6 derivative inclusion in lipid vesicles was more than 90% for DME and more than 85% for TME.

Absorption and luminescence spectroscopy. The spectral characteristics of chlorins were investigated using an SFL-1211A spectrofluorometer (SOLAR, Belarus) and a PV1251C spectrophotometer (SOLAR, Belarus).

The concentration of Chl e_6 in acetone solution was assessed from the optical density at a wavelength of 664 nm; the molar extinction coefficient was 50000 M^{-1} cm^{-1} L. The concentrations of DME and TME were measured at a wavelength of 666 nm; the molar extinction coefficient was 54 000 M^{-1} cm^{-1} L. To determine the concentration of the PS incorporated in lipid vesicles, liposomes were first lysed by addition of the 0.2% non-ionic detergent Triton X-100 (Panreac, Spain)

Cell culture. The K562 myeloid leukemia cell line was from the collection of cell cultures of the Belorussian Research Center of Pediatric Oncology, Hematology, and Immunology. Cells were cultured as a suspension in RPMI-1640 medium (Sigma, United States). For the experiments, cells were washed and transferred into a medium containing 5% fetal calf serum (FCS) (Sigma, United States).

To eliminate the influence of aggregation, alcohol solutions of PSs were preincubated in the RPMI-1640 medium containing 5% FCS. Chl e_6 or its derivatives in solutions at concentrations from $5 \cdot 10^{-6}$ M to $1 \cdot 10^{-5}$ M were added into the incubation mixture containing FCS and incubated in a thermostat (37°C) for 1 h. The K562 cells at $1 \cdot 10^6$ cells/mL were loaded into the prepared sample and incubated at 37°C for the required time to allow pigment accumulation and then washed three times with the medium from unbound PSs. LFs were added to cells in the RPMI-1640 medium containing 5% FCS and incubated according to the same protocol. Cells were pelleted by centrifugation and diluted with a fresh culture medium to $5 \cdot 10^6$ cells/mL.

Confocal laser scanning microscopy. Determination of intracellular chlorin localization. An analysis of PSs localization in live K562 cultured cells was performed using a TCS SPE laser scanning confocal fluorescence microscope (Leica, Germany). Cells were loaded onto SuperFrost slides and covered with cover glasses 0.17 mm thick. Immersion 63× magnification objectives lens were used. An argon laser with a wavelength of 488 nm was the fluorescence excitation source; fluorescence was recorded at 620–700 nm.

The intracellular distribution of chlorin was assessed by detecting the colocalization of the PS with organelle-specific markers. PSs were accumulated in cells according to the above-described protocol; the cells were then rinsed and resuspended in RPMI-1640 to the final concentration of $2 \cdot 10^6$ cells/mL. Next, cells were incubated with colocalizers according to standard protocols that were used to assess the intracellular localization of the studied PSs. The organelle-specific fluorescent probes were the Mito Tracker® Green FM mitochondrial probe ($\lambda_{excitation} = 490$ nm, $\lambda_{emission} = 511$ nm) at a concentration of $4 \cdot 10^{-7}$ M; the

Lyso Tracker® Green DND-26 lysosomal probe ($\lambda_{excitation}$ = 504 nm, $\lambda_{emission}$ = 511 nm) at a concentration of $1 \cdot 10^{-7}$ M; the NBD-,BODIPY-Labeled Sphingolipids marker ($\lambda_{excitation}$ = 505 nm, $\lambda_{emission}$ = 511 nm) at a concentration of $5 \cdot 10^{-6}$ M was colocalizer for Golgi complex; ER Tracker® TM Green ($\lambda_{excitation}$ = 504 nm, $\lambda_{emission}$ = 511 nm) at a concentration of $1 \cdot 10^{-6}$ M was colocalizer for endoplasmic reticulum.

The fluorescence intensity of colocalizers was measured in a channel in the range of 505–550 nm emission wavelength. The fluorescence of PSs was recorded in another channel (620–700 nm). Superposition of fluorescence images from two channels made it possible to compare the intracellular distribution of the probe and the PS. The degree of colocalization was estimated quantitatively using the Pearson correlation coefficient (PCC) according to [10].

A computer-assisted analysis of the fluorescence images and quantitative analysis of the parameters of PS intracellular accumulation and distribution were performed using the ImageJ software.

Cytofluorometric analysis. determination of cell damage mechanisms. Changes in cells induced by photodynamic exposure were analyzed using an FC 500 cytofluorometer (Beckman Coulter, United States). The mean fluorescence intensities of cell populations were calculated for particular time intervals using the CXP statistical software (Beckman Coulter, United States).

The changes in cell structure during photosensitization were evaluated from distribution of cells by lateral and forward light scattering intensities. In the study of apoptosis dynamics, data of light scattering were fitted to changes in the fluorescence of propidium iodide, a dye which intercalates in the DNA helix, as well as to changes in the fluorescence of a lipophilic fluorochrome chloromethyl-X-rosamine (CMXRos; Mito Tracker® Red), which is used to measure mitochondrial membrane potential.

To assess photosensitization mechanisms, K562 cells were cultured in media with different contents of DChl e_6 or their LFs for 1 h (3 h for TME) at 37°C, washed twice from unbound PSs, resuspended in a fresh medium and irradiated with a diode laser (λ = 660 nm) with controlled radiation power (ILM-660-0.5; LEMT, Belarus). Photoirradiation was carried out for 20 s at room temperature. The final light dose was 0.4 J/cm^2. The cells were then placed in a thermostat at 37°C. Two series of the samples were prepared: aliquots of cell suspension were taken at regular intervals (30 and 180 min) to count damaged cells (necrosis or late apoptosis) in an analysis of cell viability using propidium iodide (the final concentration was 1 μg/mL), as well as in a test using CMXRos (the final concentration was 150 nM) to assess early apoptotic alterations. Propidium iodide or CMXRos were added to cells 5 min and 25 min prior to cytometry, respectively. Incubation with the fluorochromes was included in the total incubation time. Under the dark regime, the addition of CMXRos at concentrations up to 250 nM did not lead to additional cell death.

A 620 nm narrow-band optical filter was used to measure the fluorescence level of dyes using a cytofluorometer. Fluorescence excitation wavelength was 488 nm (a single-phase argon laser).

Dark cytotoxicity of PSs was assessed in the MTT assay according to the protocol described in [11].

RESULTS

The localization and accumulation of the tested PSs were analyzed basing on their fluorescence characteristics in cells.

The photophysical and spectral-fluorescent characteristics of chlorins. It has been shown that Chl e_6 and its monomeric esterified derivatives in solutions of organic solvents are similar in their spectral and fluorescent characteristics [12]. Major band positions of the studied monomeric chlorins differed by 1–2 nm in absorption and fluorescence spectra. Esterification of side substituents significantly changes the polar properties of chlorin molecules, which decreases their solubility and, consequently, leads to aggregation in aqueous solutions. This causes differences in the fluorescence parameters of Chl e_6 and its esterified derivatives in aqueous solutions. To illustrate, while the fluorescence characteristics in organic solvents for Chl e_6 and its derivatives were similar, the values of their quantum yields and fluorescence lifetimes changed significantly as the chlorines were transferred into a phosphate-salt buffer. The fluorescence quantum yield for Chl e_6 when transferred into aqueous medium changed from 19.2% in acetone to 5.5% in phosphate-buffered salt solution and from 18.0 and 18.2% in acetone to 1.3 and 1.1% in phosphate-buffered salt solution for DME and TME, respectively. The fluorescence lifetimes (τ) for Chl e_6 and its derivatives DME and TME in acetone were 5.32, 5.21, and 5.23 ns, respectively. Upon transfer into phosphate-salt buffer, the value of τ was 4.53 ns for Chl e_6, 2.4 ns, for DME, and the τ value was not determined for TME [12–14].

The incorporation of DChl e_6 in liposomes preserves the monomeric state of the PSs in an aqueous medium. The fluorescence quantum yield and fluorescence lifetime for DChl e_6 encapsulated in lipid vesicles were close to the maximum value, which is characteristic of pigment solutions in organic solvents [12]. Thus, the fluorescence quantum yield was 16.9 and 17.1% for liposomal forms of DME and TME; the fluorescence lifetime was 5.12 and 5.22 ns, respectively. There were no significant differences in the nature of the electronic absorption and fluorescence spectra of DME and TME in ethanol and in DMPC

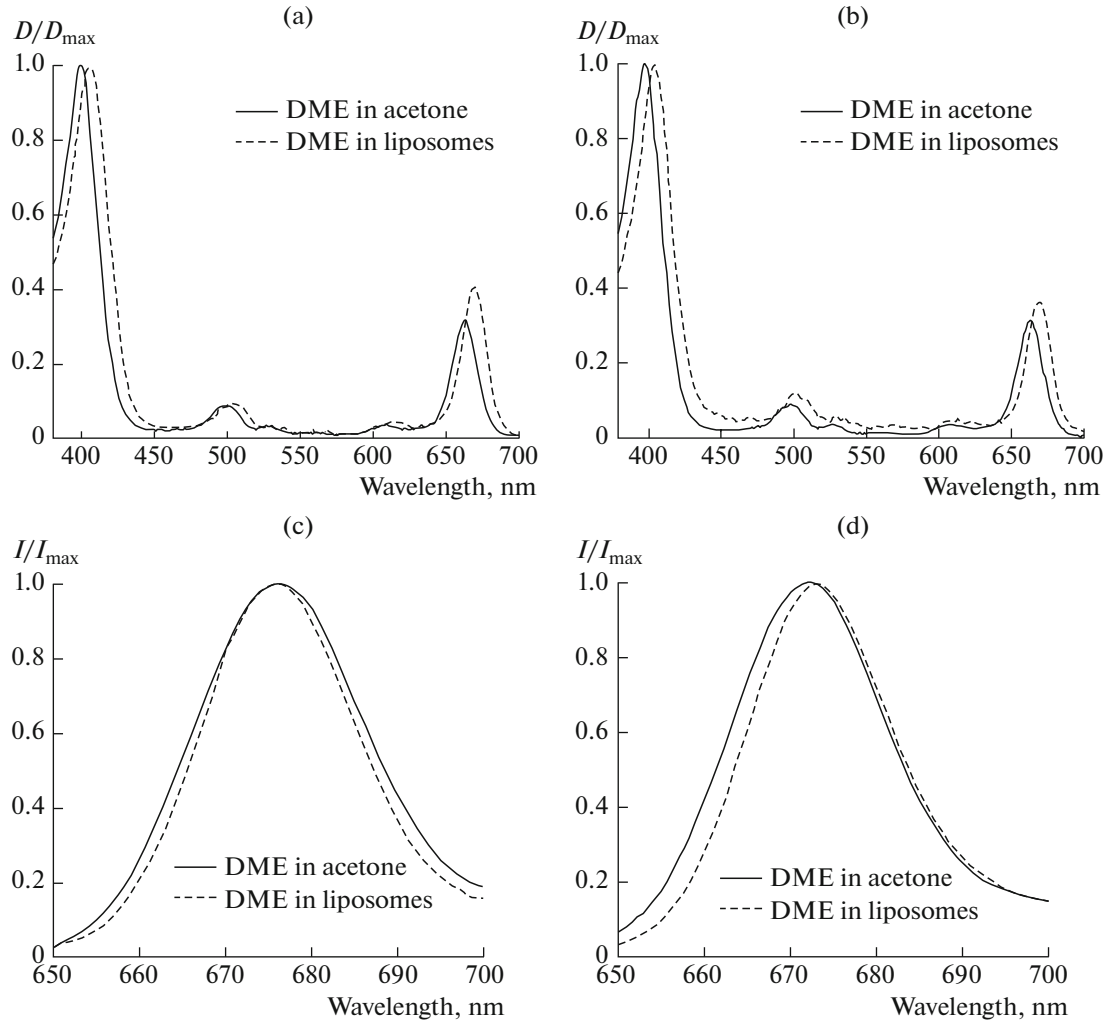

Fig. 2. The electronic absorption spectra of (a) DME and (b) TME and fluorescence spectra of (c) DME and (d) TME in ethanol and extruded DMPC liposomes in a solution of phosphate salt buffer. The concentration of DME and TME for electronic absorption spectra was $5 \cdot 10^{-6}$ M; the concentration of DME and TME for fluorescence spectra was $2 \cdot 10^{-7}$ M. The DME (TME) : DMPC ratio was 1 : 40.

liposomes (Fig. 2). The spectral-fluorescence characteristics of DME and TME in the composition of LFs prepared by extrusion technique almost did not change with an increased degree of load within the 1 : 1000–1 : 100 range.

Therefore, the photophysical and spectral-fluorescent characteristics of Chl e_6 and its esterified derivatives in the composition of liposomes upon binding to membrane structures were similar and can be used to assess the accumulation and distribution of PSs in the cell.

Intracellular localization and accumulation of chlorin after administration in solutions or in liposomal forms. The localization and accumulation of PSs was investigated by an analyzing the distribution of their fluorescence intensity in K562 cultured cells. The first minutes of cell incubation with Chl e_6 led to fluorescence emission predominantly from the plasma membrane; Chl e_6 fluorescence levels greater than cell autofluorescence were detected only in 10–12 min of cytoplasm staining. The distribution of Chl e_6 was relatively uniform in the cytoplasm. In the case of DME and TME, the fluorescence intensity of the cells was noticeably higher as early as after a short incubation time. Furthermore, the pattern of intracellular distribution was significantly different: individual regions with fluorescence intensity that were an order of magnitude higher than cytoplasm average were revealed for TME. DME demonstrated the highest rate of accumulation, bright fluorescence, and a relatively uniform distribution in the cytoplasm (Fig. 3).

It is interesting to compare the processes of intracellular accumulation and localization of esterified DChl e_6 when administered in solution and in LFs. Figure 4 shows images of K562 cells in fluorescent light after staining with DME, TME and DME–

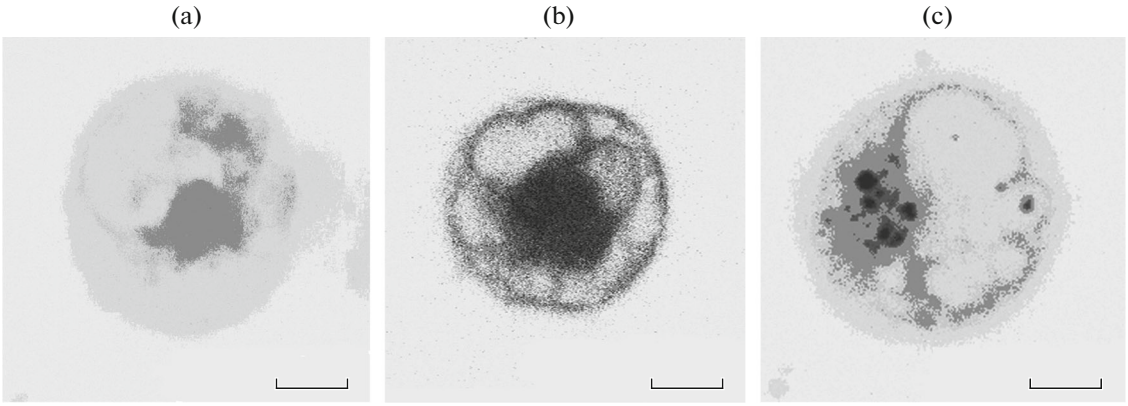

Fig. 3. Images of K562 cells in fluorescent light of chlorin (inverted): (a) Chl e_6; (b) DME; (c) TME. The pigment concentration was $5 \cdot 10^{-6}$ M; the FCS concentration was 5% in incubation medium, the incubation time was 60 min. Sections of cells are shown for $Z = 10$. The number of sections $Z = 20$, the step size was 1 μm. The scale segment on all images was 5 μm.

DMPC, and TME–DMPC complexes. Figure 4 shows that DME and TME administered in liposomes were localized as free pigments in the plasma membrane, the cytoplasm, and membrane structures. After 30-min incubation, a higher level of fluorescence for DME and DME in LFs compared to TME and its LFs was observed. The distribution of DME incorporated in liposomes was relatively uniform in the cytoplasm. The distribution pattern of TME administered in LFs within the cell body differed significantly. Similar to TME administrated in solution, individual regions with a fluorescence intensity significantly higher than the cytoplasm average were observed for TME in LF. After 90 min of incubation, the fluorescence intensity of TME increased significantly; however, the level of fluorescence intensity remained lower compared to DME. Notably, there was no fluorescence in the region of the cell nucleus for both the studied chlorins and their LFs.

An analysis of the integral fluorescence from single cells showed that when incubated for 2 h under the same conditions, the studied PSs introduced into K562 cell suspension in solutions and in DMPC liposomes have different levels of intracellular accumulation (Table 1).

The intracellular localization of the chlorins and their LFs was identified using colocalizers of cellular organelles. In the K562 cells, we compared the distribution of fluorescence from the PSs and fluorescence from organelle-specific colocalizers of endoplasmic reticulum, mitochondria, Golgi complex, and lysosomes. Figure 5 shows an example of K562 cell images when staining with DME (cells in fluorescent light from DME), the image of cells in fluorescent light from colocalizers, and the combined fluorescence of the cells after superposition of two fluorescence registration channels. The intracellular distribution of DME fluorescence moderately correlated with the distribution of fluorescence from endoplasmic reticulum and Golgi complex probes and to a lesser extent coincided with mitochondrial probe fluorescence, indicating a possible localization of DME in these organelles. It is noted that there was practically no overlap between the fluorescence regions of DME and the lysotracker.

The significance of the coincidence in the chlorin and colocalizer localization in individual organelles was assessed using the Pearson test. The values of Pearson correlation coefficients, which quantitatively characterize the degree of colocalization of the studied chlorins and their LFs with organelle-specific markers in K562 cells are shown in Table 2.

The colocalization level of Chl e_6 with mitochondria has a moderate correlation (PCC in the region of 0.5); a high level of its colocalization with endoplasmic reticulum and Golgi complex probes (PCC > 0.7) was detected. Chl e_6 accumulated in lysosomes (PCC = 0.3–0.4) to the lowest extent.

Table 1. Accumulation of Chl e_6 and DChl e_6 in K562 cells administered into a cell suspension as a solution or in liposomes

Photosensitizer	Chl e_6	DME	TME	DME–DMPC	TME–DMPC
Integral fluoresence intensity	72.6 ± 6.0	610.4 ± 24.3	340.4 ± 16.7	320.2 ± 16.1	170.4 ± 12.2

The cell concentration was $1 \cdot 10^6$/mL; the chlorin concentration was $5 \cdot 10^{-6}$ M; the FCS concentration was 5% in incubation medium. The incubation time was 120 min; the incubation temperature was 37°C. The pigment: DMPC ratio was 1 : 40. The error was estimated for three identical experiments.

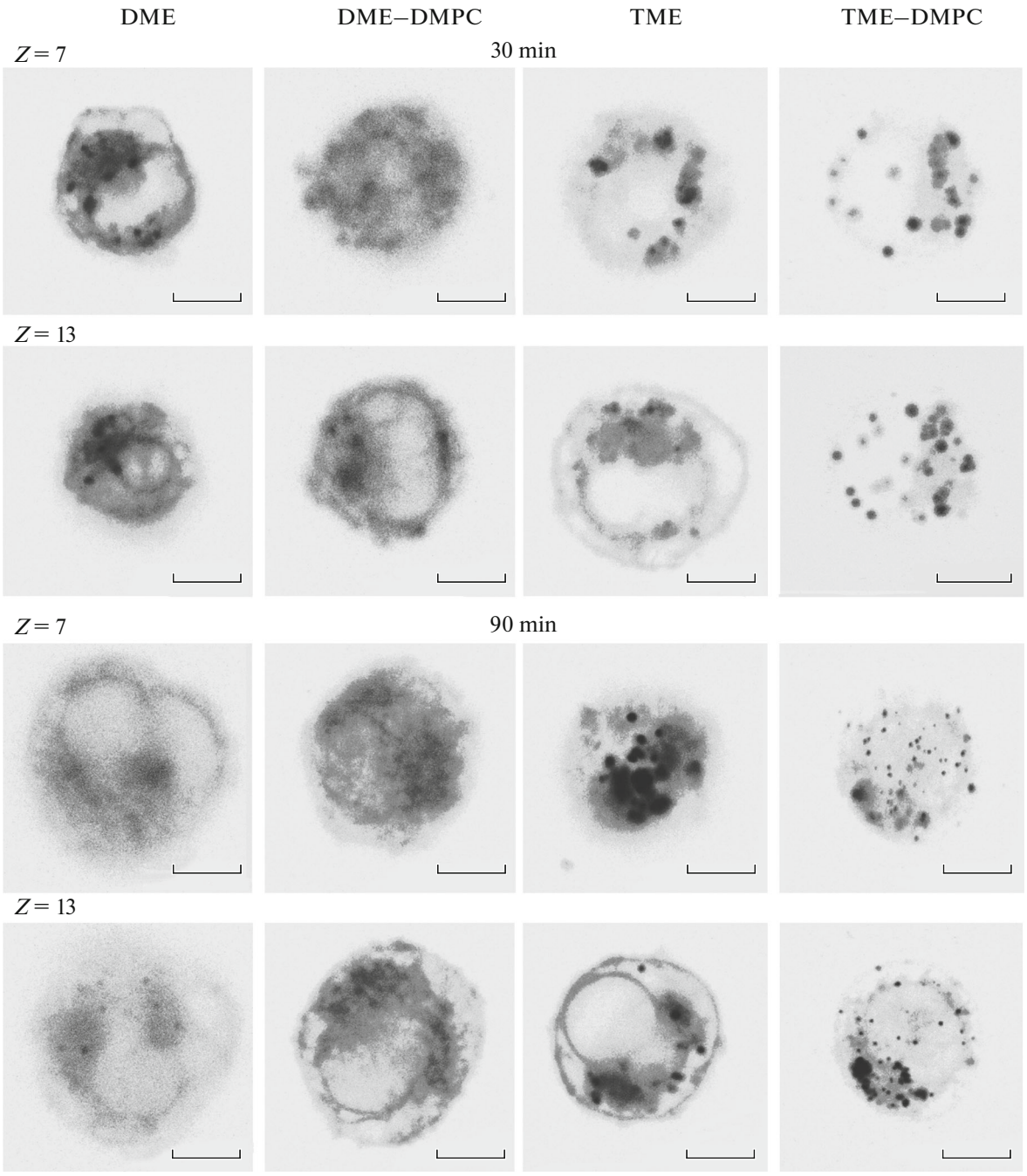

Fig. 4. Images of K562 cells stained by DChl e_6 and their liposomal forms in fluorescence imaging mode (inverted) in 30 and 90 min of incubation. The pigment concentration was $1 \cdot 10^{-5}$ M; the FCS concentration was 5%. Sections of are shown for $Z = 7$ and $Z = 13$, the number of sections Z was 20. The DMPC pigment ratio was 1 : 40. The scale of the segments on all images was 10 μm.

The data show that the esterified DChl e_6 and their LFs have the same distribution: there is a high probability of overlap between the fluorescence regions of DChl e_6 and their LFs in the cell with fluorescence of the endoplasmic reticulum probe (PCC ≥ 0.7) and Golgi complex (PCC from 0.5 to 0.7). The fluorescence regions of DChl e_6, their LFs, and mitochondrial probe coincided in a moderate manner (PCC > 0.6). There was a very weak correlation between the fluorescence regions of lysosomal probes and DME, TME, and their LFs (PCC = 0.34–0.40), which indicates a low level of DChl e_6 accumulation and their LFs in lysosomes.

Evaluation of the mechanisms involved in phototoxicity of esterified Chl e_6 derivatives and their lyposomal forms. A comparison of the ability of PSs to sensitize

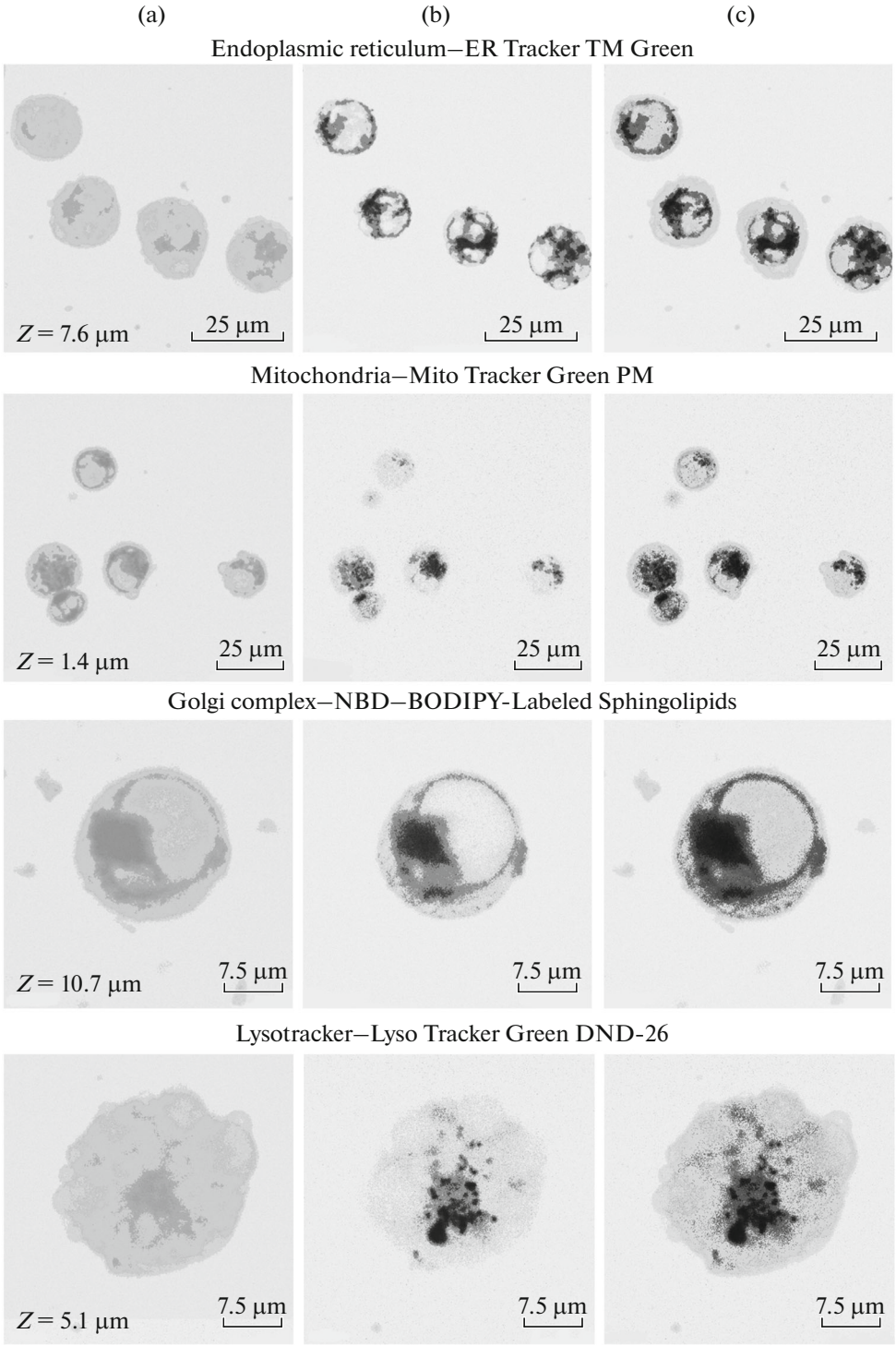

Fig. 5. A confocal image of K562 cells (inverted) stained by the DME–DMPC complex (1 : 40) (a) in fluorescent light with DME; (b) in fluorescent light with colocalizers; (c) integrated fluorescence of cells after superimposition of two fluorescence registration channels (a and b).

nectrotic and apoptotic cell damage is a subject of significant interest in investigating the influences of different types and forms of the PS administration on its activity.

Evaluation of cytotoxicity of the studied PSs and their LFs in the MTT test showed that the K562 cell viability was not affected by chlorins in concentrations from $2 \cdot 10^{-7}$ to $1 \cdot 10^{-5}$ M in non-irradiated cells. The photo-irradiation at a dose of 0.5 to 2 J/cm^2 in the absence of the PSs also did not enhance cell death.

The efficiency of the photosensitization effect on cells was evaluated after photo-irradiation a suspen-

Table 2. The Pearson correlation coefficients for Chl e_6, esterified DChl e_6, their LFs and organelle-specific colocalizers in K562 cells

PS	Pearson correlation coefficients for different cellular compartments			
	mitochondria	endoplasmic reticulum	Golgi complex	lysosomes
Chl e_6	0.517 ± 0.073	0.905 ± 0.081	0.802 ± 0.072	0.386 ± 0.046
DME	0.641 ± 0.059	0.820 ± 0.073	0.866 ± 0.079	0.380 ± 0.048
DME–DMPC	0.684 ± 0.061	0.852 ± 0.074	0.744 ± 0.067	0.400 ± 0.051
TME	0.652 ± 0.058	0.684 ± 0.069	0.560 ± 0.058	0.340 ± 0.041
TME–DMPC	0.664 ± 0.061	0.676 ± 0.058	0.520 ± 0.057	0.361 ± 0.043

The incubation time during accumulation of the PS was 3 h; the chlorin concentration was $5 \cdot 10^{-6}$ M; the FCS concentration was 5% in incubation medium. Staining with colocalizers was performed according to the protocol. The PCC value from 1.00 to 0.70 indicates a strong correlation, 0.69–0.36 is moderate correlation, 0.35–0.20 is weak correlation, less than 0.20 indicates that there is no correlation [15].

sion of K562 cells loaded with Chl e_6, DChl e_6 or their LFs by cytometry with CMXRos and fluorescent DNA dye propidium iodide.

Using the above-described methods, we compared the efficiency of photodamage of K562 cells during sensitization with chlorins and their LFs (Fig. 6). When DChl e_6 and their LFs were used as photosensitizers, the degree of both necrotic and apoptotic damage of K562 cells 30 min after irradiation was higher compared to Chl e_6 (Fig. 6a). In 3 h of incubation, the number of apoptotic cells increased by 1.5 times for Chl e_6 and by 2.1, 2.8, 2.6, and 2.4 times for DME, DME in liposomes, and TME and TME in liposomes, respectively. A comparison of the photosensitization efficiency showed that the yield of necrotic cells for DChl e_6, their LFs was also higher compared to Chl e_6. The highest efficiency of apoptotic cell damage induced by photosensitization was observed for DME and DME in liposomes.

DISCUSSION

Our results show that the chemical modification of the well-known photosensitizer Chl e_6 by successive esterification of the side carboxyl groups has an ambiguous effect on the accumulation rate of DChl e_6 in cells. The use of LFs to administer esterified DChl e_6 almost did not affect the accumulation kinetics of these PSs in cells; meanwhile, the increased number of binding centers associated with administration of DChl e_6 by of liposomes was accompanied by a decreased level of the PS accumulation (Table 1). According to our data, the studied PSs were ranked as follows according to their accumulation level in K562 cells: DME > TME > DME in liposomes > TME in

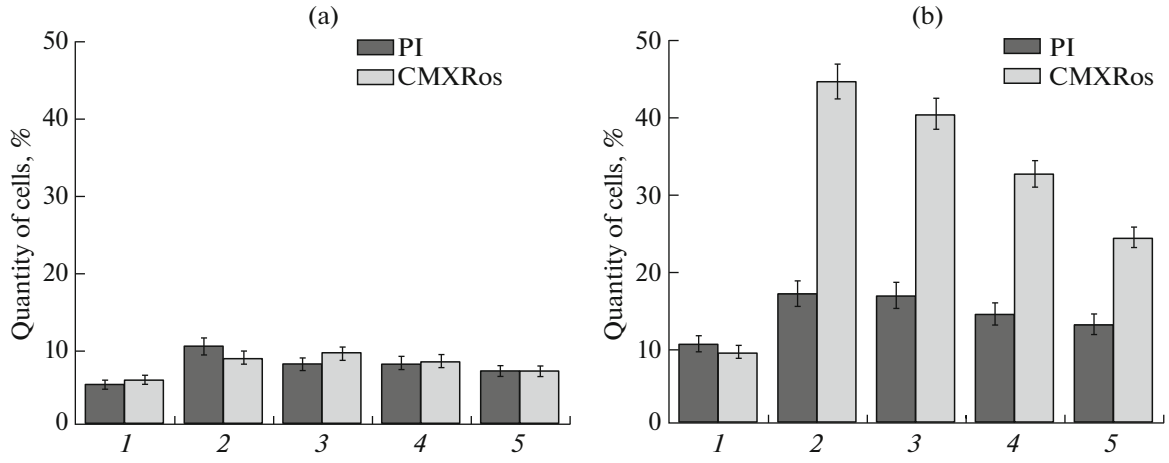

Fig. 6. The relative contents of apoptotic (test with CMXRos) and necrotic (test with propidium iodide) cells upon photosensitization with Chl e_6, DChl e_6 and their LFs with incubation time after photoirradiation of (a) 30 min and (b) 180 min. (*1*) Chl e_6; (*2*) DME; (*3*) DME–DMPC; (*4*) TME; *5*, TME–DMPC. Concentration of K562 cells was $1 \cdot 10^6$/mL. The total number of cells in the sample was taken as 100%. The DME (TME) : DMPC ratio was 1 : 40; the chlorin concentration was $2 \cdot 10^{-7}$ M; the serum concentration was 2% in incubation mixture. The light dose was 0.4 J/cm^2, $\lambda = 660$ nm. The mean values and the error of the mean ($M \pm m$) are given for three independent experiments.

liposomes ⩾ Chl e_6. Differences in intracellular accumulation rates of DChl e_6 were not associated with an aggregation effect of PSs in the extracellular medium: for pigment monomerization, non-polar PSs in solutions were administered into the culture medium with the FCS for 60 min before the cells were added.

Previous studies using the Raji leukemic cell line, peripheral blood mononuclear cells, and leukemic cells of patients with acute lymphoblastic leukemia and acute myeloid leukemia showed that the main factors that influence the accumulation level and efficiency of sensitization to cellular damage were associated with differences in the PS redistribution rates from serum proteins and nanocarriers into the plasma membrane, as well as the rate of the PS transmembrane transfer [13–16]. According to [14, 17], an increased esterification degree of the lateral groups of Chl e_6 results in significant differently directed changes of these kinetic parameters. The accumulation of relatively polar Chl e_6, which can quickly redistribute from the serum proteins and bind to the cell surface, is limited by an extremely low rate of transmembrane transfer. Consequently, the fluorescence of this PS is detected in the first 15–20 min of cell staining mainly in the plasma membrane; the value of the integral fluorescence from cells incubated with Chl e_6 is significantly lower than that observed for DME and TME stained cells. The main factor that controls the accumulation rate of TME in cells is its low dissociation rate from complexes with milieu proteins or lipid vesicles [18]. The moderately nonpolar DME, with high permeability in membrane structures and relatively high diffusion in the extracellular medium, has a maximum efficiency of intracellular accumulation.

The localization of PSs in a cell is an important determinant of effective cell damage. The use of colocalizers for various cellular organelles made possible the analysis the intracellular distribution of DChl e_6. The values of the Pearson correlation coefficients between the fluorescence of DME, TME, DChl e_6 in LFs and the mitochondrial probe fluorescence, as well as colocalizers of the endoplasmic reticulum and Golgi complex indicate the predominant localization of the PSs and their LFs in these cellular compartments. An investigation with the lysosomal probe showed a low level of correlation between the fluorescence of lysosomal probes and the fluorescence of DChl e_6 and their LFs. Therefore, it is assumed that the processes of endocytosis do not play an important role in the accumulation of both DChl e_6 and their LFs.

The ability of PSs to be accumulated in individual cell structures and the modes of photo-irradiation significantly influence the type of a mechanism involved in photosensitized cell damage [1, 19].

The results obtained in an investigation of K562 cells sensitization with DChl e_6 confirm that the PS accumulation level correlates with the relative efficiency of cellular photodamage. The percentage of damaged cells in the samples with Chl e_6 was 3.0 and 2.5 times lower compared to DME and TME, respectively. In samples containing LFs of DME and TME, the percentage of cells that underwent necrosis remained unchanged within the statistical error compared to free DChl e_6. A significant feature of K562 cells photodamage when using the PS Chl e_6 and its derivatives is the difference in the relative yield of cells undergoing apoptosis and necrosis. When using Chl e_6, the relative number of damaged cells assessed in tests with propidium iodide and CMXRos was similar. Upon irradiation of cells in the presence of DME, TME, and their LFs, the percentage of apoptotic cells significantly exceeded the percentage of cells with the plasma membrane damage (necrotic changes). Our results on the differences in the photosensitization mechanisms of cellular damage triggered by Chl e_6 and its derivatives were in full agreement with data on the degree of expression of phosphatidylserine, a marker phospholipid exposed to the outer plasma membrane of apoptotic cells. Photosensitization of cultured leukemic cells with DChl e_6 in patients with acute lymphoblastic leukemia resulted in a 2.5–4.0-fold increase in the number of Annexin V-positive cells compared to Chl e_6 [17].

The differences in the cellular mechanisms involved in photocytotoxicity of Chl e_6 and its derivatives are not related to different intensities of the photosensitization effect on cells due to different quantity of the photosensitizers accumulated in the cells. A 3–10-fold decrease in the concentration of DME and TME in cell suspensions results in cellular photodamage mostly via apoptosis (the data are not shown).

It is noteworthy that the main photophysical characteristics of all studied monomeric compounds almost coincided, including that of PS encapsulated in liposomes. Under the selected experimental conditions, Chl e_6 and its derivatives almost did not display any differences in generation of singlet oxygen, which is the main photochemical intermediator of cellular damage [12, 14]. It is suggested that the distinct mechanisms of damage were related to the features of intracellular localization and, consequently, the different targets of the photosensitization effect elicited by the studied PSs in cells. Therefore, the differences in the localization of Chl e_6 and its derivatives in mitochondria need to be taken into account. Several experimental data indicate that photosensitization exposure on mitochondria primarily activates the apoptotic pathways of cell death [15, 20]. The increased affinity of DChl e_6 to mitochondria with a higher overall level of accumulation in cells provides a much higher intensity (degree) of the sensitization effect on these organelles and, hence, predominant death of cells via apoptosis.

CONCLUSIONS

(1) The physico-chemical properties of PSs and the pharmacological formulations for their administration affect the level and the accumulation kinetics of the PSs in cells.

(2) Liposomal formulations prevent the aggregation of chlorins without a decrease their photosensitization activity.

(3) Esterified derivatives of Chl e_6: DME and TME and their LFs, are mainly localized in the endoplasmic reticulum and Golgi complex, as well as having moderate localization in mitochondria. The mitochondrial probe and Chl e_6 had a lower value of PCC compared to its derivatives and their LFs. Chl e_6, its derivatives and their LFs demonstrated a low level of localization in lysosomes.

(4) The differences in the mechanisms of cellular damage induced by Chl e_6, its derivatives and their LFs are related to different vectorization (direction) of the sensitization action of the studied PSs in K562 cells: a higher apoptotic activity of DChl e_6 and their LFs compared to Chl e_6 was linked to differences in the level of accumulation within mitochondria.

FUNDING

This study was supported by the Belarusian Republican Foundation for Basic Research, project no. B17-106.

COMPLIANCE WITH ETHICAL STANDARDS

The authors declare that they have no conflict of interest. This article does not contain any studies involving animals or human participants performed by any of the authors.

REFERENCES

1. Y. Li, Y. Yu, L. Kang, and Y. Lu, Int. J. Clin. Exp. Med. **7** (12), 4867 (2014).
2. A. A. Krasnovskii Jr., in *Problems of Regulation in Biological Systems*, Ed. By A. B. Rubin (Moscow–Izhevsk, 2006), pp. 223—244 [in Russian].
3. M. H. Teiten, L. Bezdetnaya, P. Morliere, et al., Br. J. Cancer **88**, 146 (2003).
4. H. Abrahamse, M. R. Hamblin, Biochem. J. **473**, 4, 347 (2016).
5. V. P. Zorin, V. P. Savitskiy, and M. P. Potapnev, Exp. Oncol. **24**, 142 (2002).
6. T. E. Zorina, A. A. Dalidovich, L. N. Marchenko, et al., Oftal'mol. Vost. Evropa **4**, 93 (2011).
7. M. K. Riaz, M. A. Riaz, X. Zhang, et al, Int. J. Mol. Sci. **19**, 195 (2018).
8. L. A. S. Abu and T. Ishida, Biol. Pharm. Bull. **40**, 1 (2017).
9. H. Fischer and H. Orth, *Die Chemie des Pyrrolis* (Acad. Verlag, 1937).
10. R. Taylor, J. Liagn. Med. Sonogr. **6**, 35 (1990).
11. A. P. Shpakova, K. S. Pavlova, and T. I. Bulycheva, Immunologiya **2**, 20 (2000).
12. T. E. Zorina, I. V. Yankovsky, I. E. Kravchenko, et al., Biophysics (Moscow) **60**, 759 (2015).
13. V. P. Zorin, I. I. Khludeyev, T. E. Zorina, et al., Proc. SPIE. Lazer Use in Oncology II **4059**, 139 (2000).
14. V. P. Zorin, I. I. Khludeev, and T. E. Zorina, Biophysics (Moscow) **45**, 305 (2000).
15. E. Bastein, R. Schneider, S. Hackbarth, et al., Photochem. Photobiol. Sci. **14**, 2203 (2015).
16. V. P. Savitskii, V. P. Zorin, M. P. Potapnev, and A. Ya. Potapenko, Bull. Exp. Biol. Med. **138** (2), 158 (2004).
17. V. P. Savitskii, Candinate's Dissertation in Biology (Minsk, 2008).
18. V. P. Zorin, I. S. Mikhalovsky, T. E. Zorina, et al., Biofizika **40**, 328 (1995).
19. I. O. Basselar, T. M. Tsubone, C. Pavani, and M. S. Baptista, Int. J. Mol. Sci. **16**, 20523 (2015).
20. J. Wu, Q. Xiao, Na Zhang, et al., Photodiagn. Photodyn. Ther. **15** (2016).

Translated by M. Novikova